Available online at www.sciencedirect.com

ScienceDirect

IFAC PapersOnline CONFERENCE PAPER ARCHIVE

IFAC PapersOnLine 59-23 (2025) 44–49

Long-term assessment of event-based communication for irrigation control in a bell pepper farm ⋆

L. Orihuela [*,**] **J. Bareiro** [***] **F. Reales** [*] **P. Millán** [****]

[*] *Centro de Investigación en Tecnología, Energía y Sostenibilidad, Universidad de Huelva, 21819, Huelva, Spain (e-mail: luis.orihuela@diesia.uhu.es).*

[**] *Dept. Ingeniería Electrónica, Sistemas Informáticos y Automática, Universidad de Huelva, 21007, Huelva, Spain*

[***] *Fundación Alter Vida, Itapua 1372, Asunción, Paraguay. (e-mail: jbareiro@altervida.org.py)*

[****] *Dept. Ingeniería, Universidad Loyola Andalucía, 41704, Dos Hermanas, Sevilla, Spain (e-mail: pmillan@uloyola.es)*

Abstract: This work describes the development and implementation of an event-based hysteresis controller for irrigation systems. Transmission of information from the farm is triggered attending to the instantaneous and accumulated change of moisture in the soil. The proposed methodology is assessed in a 3-month experiment in a bell pepper farm, which covers almost the entire agricultural campaign of this crop. The infrastructure, designed ad-hoc to test the methodology, consists in: edge sensing devices with capacitive soil moisture and irrigated volume sensors, edge device to actuate the electrovalve, LoRa communication, and cloud services for receiving and storing data, and for computing the control commands. The event-based policy is compared with a periodic scheme, achieving a reduction of 77% of transmissions, and increase of 11% in the battery lifespan, and achieving communication events with 4 times as much information transmitted. The hysteresis control yields a reduction of 9% of the water consumption compared to the manual irrigation of the farmer.

Keywords: Irrigation control, Event-based Control, Hysteresis Control, Precision Farming, Control in Agriculture.

1. INTRODUCTION

Although fresh water is used in almost every productive sector, agriculture is the one making the most intensive use of this resource, being responsible for nearly 70% of global freshwater consumption [1].

Traditional irrigation systems range from totally manual to fully automated operation using irrigation programmers. The programmers control irrigation in a time-based manner, choosing a time slot for each irrigation sector, that is decided based on practitioner experience or evapotranspiration models (Haghverdi et al. (2021); Rozenstein et al. (2023)). Although evapotranspiration can be refined periodically using measured variables, such as climate stations, or drainage lysimeters (Lozano et al. (2016)), these methodologies do not introduce continuous feedback of variables that affect the irrigation, such as soil moisture.

In contrast, sensor-based irrigation systems arise to partially solve this issue. By a continuous monitoring of the conditions in the soil and weather, these controlled irrigation systems have shown improvements in terms of water usage with similar or greater productivity. For strawberries, Angelopoulos et al. (2020) used Frequency-Domain Reflectometry (FDR) sensors to measure the volumetric water content (VWC) in the soil. The irrigation control implemented an ON-OFF law that opened/closed the valves using a reference VWC. For the same crop, Orihuela et al. (2025) shown that the use of low-cost capacitive sensors with a hysteresis control law increases irrigation efficiency up to 30% in a production farm.

More complex control rules have been introduced recently. Lozoya et al. (2016) applied Model Predictive Control (MPC) using FDR sensors in a pepper farm in production. MPC has also been used by Abioye et al. (2023) to control the opening of the valves in a greenhouse of cantaloupes, showing more efficient water usage than an evapotranspiration-based control.

These sensor-based methodologies rely on a periodic update of the measured data. Periodic sampling is adequate for many systems, but is not optimal for measuring VWC. The dynamics of VWC can be divided in three regions:

⋆ This work has been partially supported by Agencia Española de Cooperación Internacional al Desarrollo (AECID) through projecs DIGITALIZACIÓN (2022/ACDE/000116) and INNOVACIÓN VERDE (2024/ACDE/001188). L. Orihuela would like to thank MICIU/AEI/10.13039/501100011033 and by European Union NextGenerationEU/PRTR through grant RYC2021-032919-I.

[1] https://www.bancomundial.org/es/topic/climate-resilient-irrigation

10.1016/j.ifacol.2025.11.761

irrigation phase, in which VWC rises very fast; gravitational phase, right after the closing of the valves, in which VWC decreases fast; and evapotranspiration phase, in which VWC decreases slowly. Periodic schemes tend to oversample the evapotranspiration phase if they want to capture the dynamics of the other two regions. This comes at a cost of battery usage, as sensors are usually battery-driven to avoid wires in the farm.

Asynchronous sampling schemes offer a solution to this problem, by transmitting only when relevant information is available. There are two main approaches: event-based and self-triggered sampling. In the former, the sensor decides wether to transmit attending to some metric related to the last transmitted data and the actual measurement. In the latter, the actuator is in charge of the triggering, using an uncertain prediction model and assessing the deviations of the predictions with respect to the last received data (further details in Heemels et al. (2021)).

Event-based MPC control has been applied for irrigation control in tomato greenhouses by Pawłowski et al. (2016) and Pawlowski et al. (2017). In those documents, short experiments (10 days) report a reduction of 20% of water usage compared to standard ON-OFF control. The experiments are conducted in an experimental greenhouse where many sensors are deployed and the control action is based on Pulse-Width Modulation, which is not available in a farm, where the valves are either opened or closed.

Self-triggered control has been reported by Lozoya et al. (2021) for a one-month experiment in pecan trees. Comparison with a time-based control showed a reduction of 85% of transmissions and a reduction of 20% of power consumption. Both this and the MPCs mentioned above need a model of the dynamic of the VWC in the soil, which is estimated, in both cases, using measured data from an experiment with time-based control. This model requires frequent calibration, which complicates its implementation for the whole agricultural campaign.

In this work, hysteresis-based control of a bell pepper farm is reported for 3 months. The transmission of information is asynchronous, using an event-based scheme, avoiding the need for a model. Although the theoretical energy savings are lower than in self-triggered control, there is a practical aspect that should not be overlooked. In agricultural applications, long-range communication protocols (LoRA, Sigfox or NB-IoT) are needed, as the distances are large, and the devices need to save energy. These protocols are designed to operate from edge to cloud, this is, from the sensor to the actuator. This way, the edge devices could be switched off between two consecutive transmissions. If the actuator (cloud) decides the next transmission for a self-trigger scheme, the edge devices must keep a time window open for reception after transmission. This additional time, which depends on how fast the actuator computes the next sampling time, increases the consumption.

The proposed event-based hysteresis control is compared with a time-based irrigation policy in terms of scheduled transmissions, energy savings, information transmitted, irrigation efficiency, water consumption, and other metrics. In the authors' knowledge, this is the first reported experiment of event-based control in a farm in production for a large agricultural campaign.

This document is organized as follows. Section 2 describes the materials, including the experimental site and the edge and cloud infrastructure. Section 3 describes the event-based transmission mechanism and the hysteresis-based control law. Results and discussion are included in Section 4. Conclusions and future works are outlined in Section 5.

2. MATERIALS

2.1 Edge-cloud infrastructure

The irrigation control system is structured with a two-layer infrastructure: edge and cloud. The edge layer comprises two kinds of nodes:

- First, a pure sensing node that measures VWC. It is based on a Cubecell HTCC-AB02 microcontroller (Heltec, China) to which a set of three SoilWatch 10 (PinoTech, Poland) capacitive sensors are connected. All three sensors are installed at a depth of 20 cm and measure soil moisture every 20 minutes. Then, the microcontroller transforms the raw readings into VWC using a soil-specific calibration (see Aranda et al. (2022) for further details). Finally, the median [2] of the three values is considered as the measured VWC. The transmission of this value is made according to the event-based scheme described later.
- Second, a sensing/actuation node, that measures irrigated water volume and actuates on the electrovalves. It is based on an End-Node LT-22222-L LoRa I/O Controller (Dragino, China), that allows to generate the digital signals to operate the valves, and includes a pulse counter to measure the output of the water meter. The water meter (Gredia, USA) produces a pulse after 0.003 liters. This node transmits information to the cloud every 5 minutes.

Figure 1 shows a picture of each node deployed in the experimental site. These nodes are connected to a DLOS8 gateway (Dragino, China) using LoRa (LoRaWAN protocol). Pure sensing nodes operate in LoRaWAN class A, which means that they might receive download data only after the transmission of data. The sensing/actuation nodes operate in class C, so they can receive opening/closing commands at any time. This choice is based on the fact that the pure sensing nodes are battery driven, but the other devices have electrical supply. Finally, communication between the gateway and the cloud layer was facilitated through a 4G network.

In the cloud layer, the data are received in a The Things Stack server (Things Industry, Netherlands). The payloads received were processed and stored in a relational database hosted on Azure (Microsoft, USA). The data is used as input for the hysteresis-based control algorithm, which is executed on Amazon Web Services (Amazon, USA). The algorithm, described in Section 3, generates the commands to be sent down to the edge layer.

2.2 Experimental site

The experiment was carried out on a bell pepper farm located in Piribebuy, in the Central Department of

[2] Taking the median allows discarding sensor malfunction or sensors affected by preferential water flow paths.

(a) Pure sensing node with moisture sensors

(b) Sensing/actuation node with valves and water meter

Fig. 1. a) Pure sensing node. The wires corresponds to the soil moisture sensors, that were installed underground; b) Control panel storing the sensing/actuation node, one electrovalve and two water meter below.

Paraguari, approximately 80 km from the capital Asunción (Paraguay). The coordinates are $25.461S, 57.0360W$. The climate in Piribebuy is characterized by high temperatures and significant humidity, especially during the summer months. The rainy season extends from late spring to early autumn, with January and February experiencing the highest precipitation levels. As fall progresses, temperature decreases and humidity slightly increases. Table 1 presents historical climate data for the period when the reported experiment is conducted.

Month	Min-Max Temp. (°C)	Avg. Humid. (%)	Precip. (mm)
Jan	18.3-42.2	70	243
Feb	19.1-40.8	75	203
Mar	17.6-38.5	72	64
Apr	15.2-35.6	78	79

Table 1. Historical climate data for Piribebuy (2024). Source: Dirección de Meteorología e Hidrología Paraguay.

The experimental farm spans an area of 18×30 meters and features a slight downhill gradient of 2.5% toward the east. Granulometric analysis indicates that the soil is predominantly sandy (86–88%), with silt constituting 7.5–12.5% and a minimal clay fraction (1.5–4%). This coarse texture results in high drainage and low water retention, significantly influencing nutrient and water availability.

Fig. 2. Aerial view of the plot with semi-shade cover. The left side corresponds to the automatic subplot and the right one to the manual subplot. The red dots indicate the position of the 3 pure sensing nodes and the yellow dot is the control panel with sensing/actuation node.

The farm was organized into 10 beds, each comprising two rows of 112 bell pepper plants. Irrigation was achieved through a 16 mm drip tape system operated at 1 bar. The emitters were spaced 20 cm apart, and provided a controlled flow rate of 1 L/h. Water was supplied to the plot by gravity from a 40-meter elevated tank.

Figure 2 presents an aerial view of the field. For the case study, the farm was subdivided into two distinct plots. The eastern section, referred to as the *manual plot*, comprises 5 beds and was irrigated manually by the farmer. In contrast, the remaining section, known as the *automatic plot*, was managed with the hysteresis-based controller. In the automatic subplot, three nodes were deployed to measure VWC and one node to control the irrigation of the automatic plot. This node also measured the irrigated water volume of both subplots. The presence of three sensing nodes provides some robustness to the implementation, but only the data from one of them is used for the control. More details are given later.

The transplantation of the bell pepper seedlings occurred on December 20, 2023. The farmer started manual irrigation on both subplots on December 20, 2023, aligning irrigation with the early stages of crop establishment. After the establishment of the crop, the event-based control on the automatic subplot was activated on January 1, 2024, and remained active until the last harvest on March 21, 2024.

3. METHODS

3.1 Event-based communication protocol

As explained in Section 2.1, sensing nodes measure soil moisture and compute the VWC every 20 minutes. Then, the measured data of a node can be written as:

$$y(t_k) = \text{VWC}(t_k), \tag{1}$$

where t_k denotes the sampling time of the k-th sample, and $t_{k+1} - t_k = T_s = 20$ minutes.

Let $l(t_k)$ denote the time instant of the last transmitted measurement at a given time t_k. Then, a transmission event occured whenever one of the next three rules is met:

- **Time-based:** Given a constant time $T_{\max}$, the node sends a VWC sample at instant t_k if:
$$t_k - l(t_k) > T_{\max}. \tag{2}$$
- **Actual change:** Given a constant threshold δ_a, the node sends a VWC sample at instant t_k if:
$$|y(t_k) - y(l(t_k))| > \delta_a. \tag{3}$$
- **Accumulated change:** Given a constant threshold δ_c, the node sends a VWC sample at instant t_k if:
$$\sum_{t=l(t_k)}^{t_k} |y(t) - y(l(t_k))| > \delta_c. \tag{4}$$

The first rule ensures that, at least, one data is received after $T_{\max}$ minutes. If the other thresholds are well defined, this rule serves as a safety mechanism, since a large absence of data can be interpreted as a damage in the node, or a broken communication link.

The second rule is crucial for the irrigation and gravitational phases, as the changes in VWC are expected to be fast. An adequate choice of δ_a impacts on the triggering of more or less transmissions in those phases.

Finally, in the evapotranspiration phase, the VWC changes very slowly and then the change in VWC between consecutive measurements may not possibly be greater than δ_a. However, the accumulated change could grow bigger than δ_c, triggering a new transmission. This accumulated change measures, somehow, the total volume of water lost by the soil. This third rule intends to keep this loss monitored.

The thresholds $T_{\max}$, δ_a and δ_c were selected empirically through extensive field testing. Multiple experiments were carried out under different irrigation and environmental conditions in order to identify values that balance the ability to detect significant soil moisture variations with energy efficiency. By tuning these parameters, we aim to reduce unnecessary transmissions—thus extending the lifetime of the node—while still capturing the relevant events needed for effective irrigation monitoring.

3.2 Hysteresis irrigation control

The hysteresis control law is inspired on that of Orihuela et al. (2025), which was designed for periodic communication. Its objective is to keep the VWC within a band, this is, between a lower limit given by the permanent wilting point and an upper limit given by the field capacity.

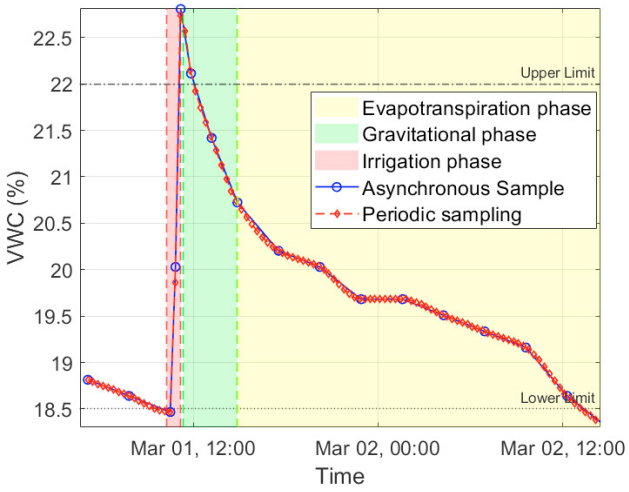

Fig. 3. Evolution of VWC during one irrigation cycle. The event-based samples are indicated with a blue circle; the periodic samplings with a red star.

The hysteresis-based controller computes the command $u(t)$ to be sent to the servovalve according to:

$$u(t) = \begin{cases} \text{CLOSE}, & s(t) = 0, \\ \text{OPEN}, & s(t) = 1, \end{cases} \tag{5}$$

where $s(t)$ is an internal dynamical state of the controller that depends on both the last received value of the VWC and the upper and lower limits. The state changes from 0 to 1 when the VWC is grows below a limit that has been chosen to avoid water stress. And it changes from 1 to 0 when the VWC crosses the field capacity.

4. RESULTS AND DISCUSSION

This section summarizes the experimental results obtained during the period from January to March 2024—a three-month study during which the automatic irrigation system operated continuously until the end of the pepper production cycle. For all the reported experiments, the parameters of the event-based triggering scheme were chosen as $T_{\max} = 180$ minutes, $\delta_a = 0.15(\%)$, and $\delta_c = 1(\%)$.

4.1 Comparison of event-based and periodic schemes

The comparison between both methods begins with a qualitative analysis of the performance of the two sampling methodologies when measuring the VWC dynamics. Figure 3 shows a complete irrigation cycle, that starts when the VWC grows below the lower limit and the servovalve opens. When the VWC crosses the upper limit, the irrigation stops and the VWC decreases during the gravitational and evapotranspiration phases. The three dynamical regions are clearly identified in the figure. It illustrates the event-triggered transmissions and all the time instants in which the node wakes up, but decides to not transmit. It is clear that the event-based capture the dynamics of the VWC.

A quantitative analysis is provided in Table 2, which accounts for the number of samples transmitted in both periodic and event-driven schemes during the entire experiment. The difference in the amount of periodic samples

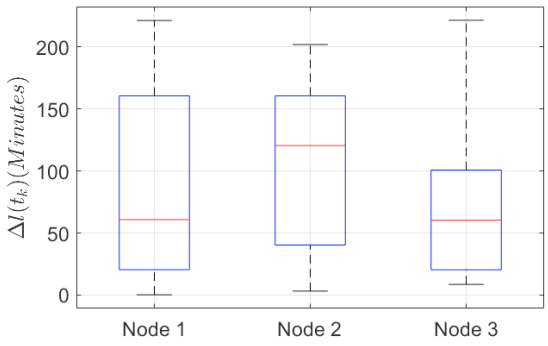

Fig. 4. Distribution of the time intervals between consecutive transmissions for the three deployed nodes. The blue box represents the interquartile range between first and third quartile, and the red line represents the median.

between nodes is due to different malfunctions. This justifies the deployment of three sensing nodes at the same depth. However, the percentage of transmitted samples with the event-based rules is similar for all the nodes. It is also similar to the reduction reported in Lozoya et al. (2021) which implemented a self-triggered scheme.

Node	Asynchronous Samples	Periodic Samples	Percentage (%)
1	1021	4087	24.982
2	796	4108	19.377
3	158	570	27.719

Table 2. Total transmissions triggered with event-based and periodic sampling schemes for each deployed node.

A deeper analysis can be performed by observing the statistical distribution of the time intervals between two consecutive transmissions, denoted with some abuse of notation as $\Delta l(t_k)$. This is shown in Figure 4 for each node. It shows that node 2 triggers most of its transmissions after 2 hours, which is close to $T_{\max}$. This may suggest that the choice of the event-based parameters are not fully adequate for the conditions of this node, as the third rule for triggering events seem to be dominant. In nodes 1 and 3, the time intervals are better distributed. This fact, together with the malfunctioning observed in node 3 (see Table 2) encouraged the use of the data incoming from node 1 to control the irrigation.

A complementary analysis can be done in terms of energy consumption. First of all, and before deployment in the farm, the energy consumption of the node is measured using a Power Profile Kit (Nordic Semiconductor, Norwey). In particular, the routine executed by the nodes is divided in stages, namely, initialization, idle (I), measure, transmission, idle (II), ACK reception, and deep sleep. Table 3 shows the average consumption of the different stages and the average time of each stage. Please note that, if no transmission is triggered, the cycle has less stages.

Using the data from Table 3, and the percentage of transmissions in Table 2, the average energy consumption can be computed as:

$$\text{Avg. Consump. (mAh)} = \alpha E_t + (1-\alpha)E_{nt},$$

where α is the percentage of transmissions, and E_t, E_{nt} is the energy consumption of the routines with and without

Stages	Time (s)	Consumption (mA)	Energy (mAh)
Routine with transmission			
Initialization	0.06	0.12277	0.000002
Idle (I)	0.368	0.01412	0.000001
Measure	1.193	57.26	0.018975
Transmission	0.169	85.89	0.004032
Idle (II)	4.892	0.02493	0.000034
ACK reception	0.109	4.29	0.000130
Deep Sleep	1193.209	0.01412	0.004680
Total	1200		0.027854
Routine without transmission			
Initialization	0.06	0.12277	0.000002
Idle (I)	0.369	0.01412	0.000001
Measure	1.198	57.26	0.019055
Deep Sleep	1198.373	0.01412	0.004700
Total	1200		0.023759

Table 3. Energy consumption for the routines executed by the node with and without transmission

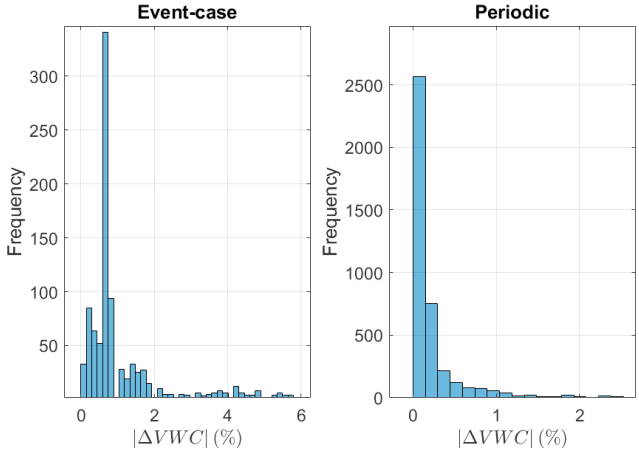

Fig. 5. Number of samples (absolute frequency) triggered classified attending to the absolute value of the change in VWC with respect to the previous transmission

transmissions. For node 1, the average consumption is 0.024677 mAh. Considering a common 4.2 V battery, with 2300 mAh, node 1 will have an average battery autonomy of 1153 days with periodic sampling and 1295 days for event-based. This represents an increase of 10.97%, equivalent to approximately 142 days additional days of autonomy. This reduction is shorter than the one reported in Lozoya et al. (2021), which reached 20%. The use of a model and more complex computations in the cloud seems to produce better results in terms of battery lifespan.

Periodic and event-based sampling can also be compared in terms of the amount of information transmitted in each new sample. This amount of information is measured with the absolute value of the change in VWC between two consecutive transmissions, denoted as $|\Delta$VWC$|$. This metric is shown in Figure 5 using a histogram.

The left histogram (event-based) shows a broader distribution of VWC changes, indicating that the samples contain different amount of information depending on the region—irrigation, gravitational, evapotranspiration—in which it was generated. The mode of this distribution is around 0.8%, which is adequate according to the VWC range observed in the cycle shown in Figure 3. In contrast, the right histogram (periodic) exhibits a highly skewed

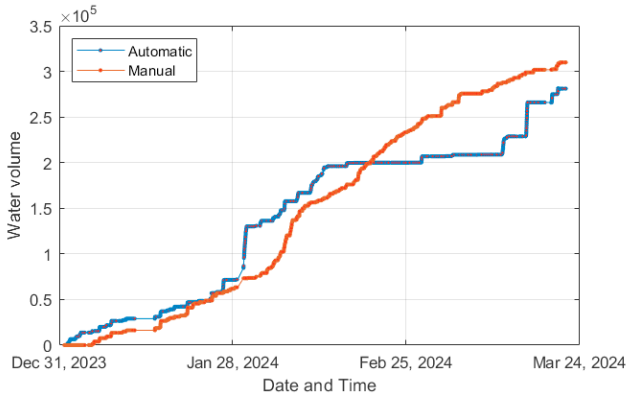

Fig. 6. Accumulated water volume over time for the automatic and manual plots.

distribution with a predominance of minimal changes of less that 0.2%, suggesting that periodic sampling often records redundant or insignificant variations.

4.2 Comparison of event-based hysteresis control and manual irrigation

The proposed control methodology is compared with the manual irrigation of the farmer in terms of water consumption.

Figure 6 shows the accumulated water volume irrigated in both subplots during the whole experiment. The total water consumed was 309878 liters for the manual plot and 281104 liters for the automatic plot. Both subplots contained 560 plants. This corresponds to a water consumption per plant of 501.97 liters for the automatic system and 553.35 liters for the manual plot, achieving a reduction of 9.3%, which is a bit smaller than the one obtained in Pawlowski et al. (2017) using MPC during a 10-day experiment in an experimental greenhouse.

5. CONCLUSIONS

This works describes the design and implementation of event-based irrigation control in a bell pepper farm. The experimental results cover almost the complete agricultural campaign, and it is included a detailed comparison with a periodic sampling scheme and the manual irrigation of the farmer. The results are encouraging in terms of reduction of transmissions (savings of 77%), energy consumption (11% increased lifespan), and water consumption (9% reduction). Some published works implementing asynchronous communication strategies reported better numbers in terms of water or energy consumption, but they required a dynamical model of the soil moisture that have to be calibrated with periodic data and, therefore, only short experiments are reported.

In the future, the application of self-triggered schemes or more complex control rules with an adaptive model is pursued. The validation with other crops and irrigation systems is also interesting.

ACKNOWLEDGEMENTS

The authors would like to acknowledge all the team involved in DIGITALIZACIÓN and INNOVACION VERDE projects, with special thanks to Alfredo Galeano for his technical support, and Daniel Pereira, for his institutional support and agronomical supervision.

REFERENCES

Abioye, A.E., Abidin, M.S.Z., Mahmud, M.S.A., Buyamin, S., Mohammed, O.O., Otuoze, A.O., Oleolo, I.O., and Mayowa, A. (2023). Model based predictive control strategy for water saving drip irrigation. *Smart Agricultural Technology*, 4, 100179.

Angelopoulos, C.M., Filios, G., Nikoletseas, S., and Raptis, T.P. (2020). Keeping data at the edge of smart irrigation networks: A case study in strawberry greenhouses. *Computer Networks*, 167, 107039.

Aranda, D., Tapia, A., and Millan, P. (2022). Calibración y caracterización de sensores capacitivos de bajo coste para la monitorización de humedad de suelo. In *XLIII Jornadas de Automática*, 479–485. Universidade da Coruña. Servizo de Publicacións.

Haghverdi, A., Singh, A., Sapkota, A., Reiter, M., and Ghodsi, S. (2021). Developing irrigation water conservation strategies for hybrid bermudagrass using an evapotranspiration-based smart irrigation controller in inland southern California. *Agricultural Water Management*, 245, 106586.

Heemels, W., Johansson, K.H., and Tabuada, P. (2021). Event-triggered and self-triggered control. In *Encyclopedia of Systems and Control*, 724–730. Springer.

Lozano, D., Ruiz, N., and Gavilán, P. (2016). Consumptive water use and irrigation performance of strawberries. *Agricultural Water Management*, 169, 44–51.

Lozoya, C., Favela-Contreras, A., Aguilar-Gonzalez, A., Félix-Herrán, L.C., and Orona, L. (2021). Energy-efficient wireless communication strategy for precision agriculture irrigation control. *Sensors*, 21(16), 5541.

Lozoya, C., Mendoza, C., Aguilar, A., Román, A., and Castelló, R. (2016). Sensor-based model driven control strategy for precision irrigation. *Journal of Sensors*, 2016(1), 9784071.

Orihuela, L., Pacheco, E., Bareiro, J., Tapia, A., and Manzano, J.M. (2025). Deployment of a smart irrigation control system with capacity-based moisture sensors on a production farm. *Journal of Irrigation and Drainage Engineering*, 151(1), 04024039.

Pawłowski, A., Sanchez, J., Guzmán, J.L., Rodríguez, F., Berenguel, M., and Dormido, S. (2016). Event-based control for a greenhouse irrigation system. In *IEEE International Conference on Event-based Control, Communication, and Signal Processing*, 1–8.

Pawlowski, A., Sánchez-Molina, J., Guzmán, J., Rodríguez, F., and Dormido, S. (2017). Evaluation of event-based irrigation system control scheme for tomato crops in greenhouses. *Agricultural Water Management*, 183, 16–25.

Rozenstein, O., Fine, L., Malachy, N., Richard, A., Pradalier, C., and Tanny, J. (2023). Data-driven estimation of actual evapotranspiration to support irrigation management: Testing two novel methods based on an unoccupied aerial vehicle and an artificial neural network. *Agricultural Water Management*, 283, 108317.